

Effects of Citral on *Aspergillus flavus* Spores by Quasi-elastic Light Scattering and Multiplex Microanalysis Techniques

Man LUO^{1,2}, Li-Ke JIANG², Yao-Xiong HUANG³, Ming XIAO⁴, Bo LI⁴, and Guo-Lin ZOU^{1*}

¹College of Life Sciences, Wuhan University, Wuhan 430072, China;

²College of Life Sciences, Anhui Agricultural University, Hefei 230036, China;

³Institute of Biomedical Engineering, Ji'nan University, Guangzhou 510632, China;

⁴Ministry of Education Key Laboratory for Biodiversity Science and Ecological Engineering, the Institute of Biodiversity Science, Fudan University, Shanghai 200433, China

Abstract Citral refined from *Litsea cubeba* oil has been found to have a strong influence on fungi, especially *Aspergillus flavus*. Multiplex microanalysis and quasi-elastic light scattering techniques were applied to study the effects of citral on *Aspergillus flavus* spores from the levels of membrane, organelle and intracellular macromolecule. It was found that citral injured the wall and the membrane of *A. flavus* spore, resulting in decrease of its elasticity. After entering the cell, citral not only influenced the genetic expression of mitochondrion reduplication and its morphology, but also changed the aggregation of protein-like macromolecules. As a result, cells, organelles and macromolecules lost their normal structures and functions, eventually leading to the loss of germination ability of *A. flavus* spores. Since *Litsea cubeba* oil as food additive and antifungal agent is safe and less poisonous, it is important to elucidate the inhibitory mechanisms of *Litsea cubeba* oil on the germination ability of *A. flavus* spore.

Key words citral; *Aspergillus flavus* spore; multiplex microanalysis techniques; quasi-elastic light scattering technique

Litsea cubeba (Lour.) Pers. is a kind of medicinal plant in China. The first report about the antibacterial and anti-phlogistic function of *Litsea cubeba* (Lour.) Pers. and its oil appeared in the *Zhong Yao Da Ci Dian* [1]. Since 1980s, many studies showed that *Litsea cubeba* oil had wide antibacterial and antifungal activity [2–4]. The antibiotic functions of *Litsea cubeba* oil are attributable mainly to citral [5–7], which amounts to 60%–80% of the essential oil [8]. Pattnaik [9] reported that citral could effectively inhibit 14 bacteria and 12 fungi. Zhou *et al.* [10] studied the antibacterial mechanism with isotope labeling. We reported that when *A. flavus* spores (AFS) were treated by citral, the germination percentage of AFS decreased remarkably, and even AFS germinated and grew, its mycelia produced no conidiospores [11]. The underlying mechanisms of the inhibitory effects of citral on the germination of AFS remain unclear.

In this study, quasi-elastic laser light scattering technique was used to determine the size and distribution of particles in the extracts of AFS treated by citral. Multiplex microanalysis techniques were used to obtain absorption spectrum from a micro region of 1 μm in living AFS cell to determine the membrane elasticity and morphological parameters of the spores. Moreover, transmission electron microscopy was employed to observe the ultrastructure of spore treated by citral and the mitochondrion in the mycelium, which germinated from AFS damaged by citral. With such data, we tried to elucidate the mechanisms of citral inhibition on AFS germination at the levels of cell, sub-cell and molecule, and to provide theoretic basis for efficient utilization of *Litsea cubeba* (Lour.) Pers..

Materials and Methods

Strain and citral

Aspergillus flavus (*A. flavus*) strain No. 3.2758 was

Received: February 1, 2004 Accepted: February 26, 2004

This work was supported by a grant from the Department of National Archives of China (No. 903-protect-02).

*Corresponding author: Tel, 86-551-2822298; Fax, 86-551-2822298; E-mail, xionglu@ustc.edu.cn

supplied by the Institute of Microbiology, Chinese Academy of Sciences. It was cultured on Potato dextrose agar (PDA; Difco, France) at 29 °C.

Citral was extracted from *Litsea cubeba* oil by distillation with a purity of 97.7% [12]. The concentrations of citral used in this study were 0.5, 1.0, 1.5 and 2.0 mg/ml of phosphate buffer (pH 7.2, containing 0.1% glycerol).

Multi-dimensional microscopy system

The system installed on an inverted microscope (Nikon TE2000) consists of three parts: a multi-channel microspectrophotometer (MCMS), a cell culture mini-chamber, and a multifunctional micro-image processor and analyzer. The system is capable of performing non-invasive, *in situ*, real time measurement on the multiple parameters of a single cell with high sensitivity. The MCMS was composed of a monochromator, a linear array CCD (charge coupled device), and a computer. With MCMS, the multi-spectrum measurement was carried on 1 μm region (350–800 nm, with a resolution of 0.2 nm). The multifunctional micro-image processor and analyzer subsystem is capable of capturing hundreds of cell frames in a few seconds. In addition to its common functions (e.g. static and dynamic analysis of point, line, area and volume), the subsystem also has some specially designed software for cell classification, measurement of the visco elastic properties of the cell membrane, and analysis of single cell gel electrophoresis (SCGE) to obtain quantitative information about the DNA damage of eukaryote.

Preparation of samples

A. flavus spores (AFSs) harvested from the culture grown in PDA medium for 5 days, were washed 3–4 times with phosphate buffer (pH 7.2) containing 0.1% Tween-20. The suspension was centrifuged at 3000 rpm for 10 min at 4 °C. The spores were collected and treated with citral solutions of different concentrations. Three hours later, the spores were centrifuged at 3000 rpm for 10 min and kept at 4 °C for use.

A. flavus mycelia (AFM) used in this study were prepared according to the following procedure. The spores from the culture grown for 5 days in PDA medium containing 0.5 mg/ml citral (minimal inhibitory concentration, MIC) were washed with physiological saline, and then inoculated onto fresh PDA medium and incubated at 29 °C for another 5 days. Finally, the ultra-structure of mycelia was examined under transmission electron microscope (Philips Tecnai 10, Netherlands) at 80 kV.

Analysis of a single living AFS with multi-dimensional microscopy system

The above prepared AFS samples were suspended in phosphate buffer (pH 7.2, containing 0.1% glycerol) to a density of 5000 spores in 1 ml, and added into the culture chamber. After 10 minutes, the multi-dimensional microscopy system was used to measure the morphological parameters of AFS, the elastic parameters of membrane (e.g. bending modulus K_c and shear modulus μ) [13,14] and the absorbance in continuous spectrum of a single living AFS [15,16]. The control group was incubated in the PB buffer for another 3 h after it was already treated by citral for 3 h.

Determination of particle diameter size of AFS extracts and its distribution

The spore sample was suspended in Tris-HCl buffer (pH 7.2) to a concentration of 10^6 spores per ml of the buffer, broken by ultrasonic apparatus (JY92-II SCIENTZ, made in China), and centrifuged at 6000 rpm, 4 °C for 45 min. The supernatant was used for the determination of the diameter size of particles and its distribution in the solution through the quasi-elastic laser light scattering instrument (BI 2000, BI9000 AT model, Brookhaven Corp., USA) [17].

Transmission electron microscope observation of AFS and AFM

The above treated AFS were embedded in 0.7% agar gel, and 1 mm tablet containing AFS was obtained by slicing. The AFS tablet and the AFMs were fixed in 0.1 M cacodylate buffer (pH 7.2, containing 3% glutaraldehyde) at room temperature for 4 h, and washed three times with cacodylate buffer, each time for 20 min. Specimens were post-fixed in cacodylate buffer containing 2% OsO_4 at room temperature for 2 h, and dehydrated in a gradual ethanol series (30%, 50%, 75%, 85%, 95%, twice at each concentration of alcohol for 20 min). Finally, they were dehydrated twice in pure ethanol (each for 1 h), embedded in Spurr resin and incubated at 65 °C for 16 h. They were trimmed, sliced and stained with uranium acetate and lead citrate, and examined under transmission electron microscope at 80 kV.

Results

Change of AFS morphology

Surface structure under optical microscope The micro-image of AFS was taken by Multi-dimensional microscopy system (with oil immersion objective, 100×) (Fig. 1). It was observed that the surfaces of the AFS treated by citral became rough in contrast to the control group. As the concentration of citral increased, some bulges occurred on the surface. Subsequently, the cell gradually became smaller. When the concentration of citral was higher than 5.0 mg/ml, the AFS were broken into pieces.

Surface structure under transmission electron microscope

Compared with the control group, when the concentration of citral was low (0.5 mg/ml), the outside wall of cell was partially shelled off. Though the wall was little expanded, its electron density was lower than that in the control, indicating that the wall structure became loose (Fig. 2). However, the electron-thin in the periplasmic space still existed. The cytomembrane was infolded markedly. When the concentration of citral was 2.0 mg/ml, most of

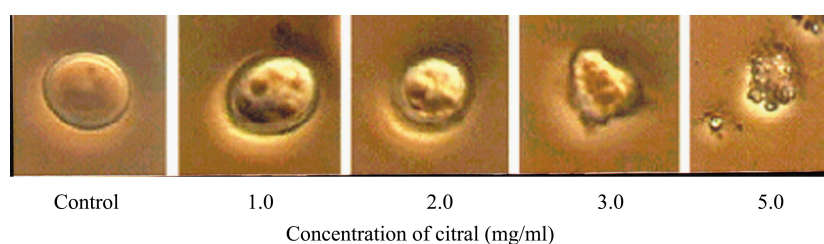


Fig. 1 Effects of citral on the surface structure of AFS
The magnification is 8000×.

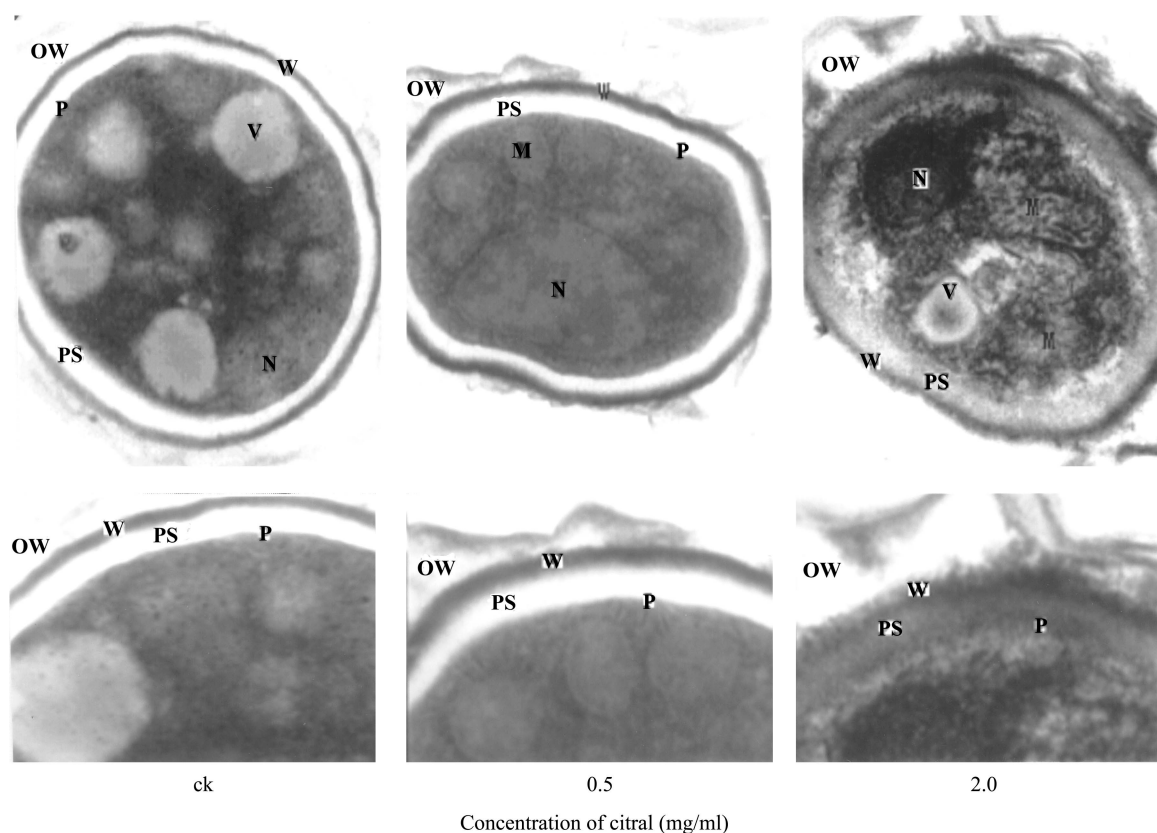


Fig. 2 Effects of citral on the wall and membrane of AFS

OW, outside wall of cell; W, the wall of cell; PS, the periplasmic space; M, the membrane; Mt, the mitochondrion; N, the nucleus; V, the vesicles. Top row pictures: magnification $\times 27,000$; bottom row pictures: magnification $\times 40,500$.

the outside cell wall was broken and the brink of wall surface become rough and villiform, and the density of its electron-dense significantly decreased. Furthermore, the AFS cytomembrane was partially collapsed or degraded and its periplasmic space became electron-dense, suggesting that the degraded product entered the periplasmic space from the wall and membrane. All above proved that citral could injure AFS wall and membrane to a certain extent.

Morphological parameters of AFS More than 200 AFSs were selected for measuring morphological parameters. Their mean values of morphological parameters (such as area, perimeter, major axis, and minor axis) were analyzed with multi-dimensional microscopy system. Compared with the control group, the parameter values of the test groups were lower, especially the values of area and perimeter (Fig. 3). It was shown that these parameters decreased with increasing concentration of citral. Similar results were obtained when spores treated with citral were retransferred to phosphate buffer without citral, so citral brought about irreversible changes of these parameters.

Elasticity of membrane The bending modulus Kc and the shear modulus μ are important elasticity parameters of membrane representing incompressibility and rigidity respectively. As Kc and μ increase, the elasticity of membrane decreases whereas the rigidity of membrane increases, that is, cell is prone to crash. At 25 °C, the elasticity parameter of membrane of a single intact AFS was measured with multi-dimensional microscopy system and

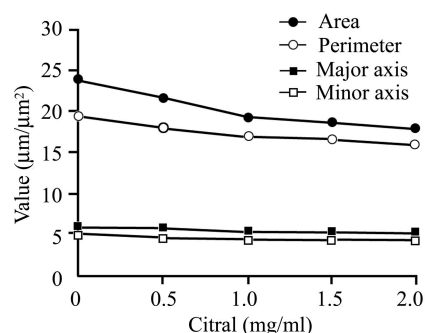


Fig. 3 Effects of citral on the morphological parameters of AFS

dynamic image analyzing technique. Regression analysis showed that a linear relationship existed between Kc and μ of AFS membrane and the concentration of citral (for Kc : $Kc=73.88+179.46 \times [\text{citral}]$, $r^2=0.99$, $P<0.001$; for μ : $\mu=-78.48+1115.67 \times [\text{citral}]$, $r^2=0.94$, $P<0.01$).

Change of mitochondrion in AFM

Luo *et al.* [18] reported that irregular proliferation, abnormal shape and disordered structures occurred in the mitochondrion (Mt) extracted from AFM damaged by citral under scanning electron microscope. Similar changes were also observed under transmission electron microscope, and the number of Mt increased. Mitochondria of irregular shapes were found in the injured AFM (Fig. 4). Therefore, citral caused changes of Mt in both

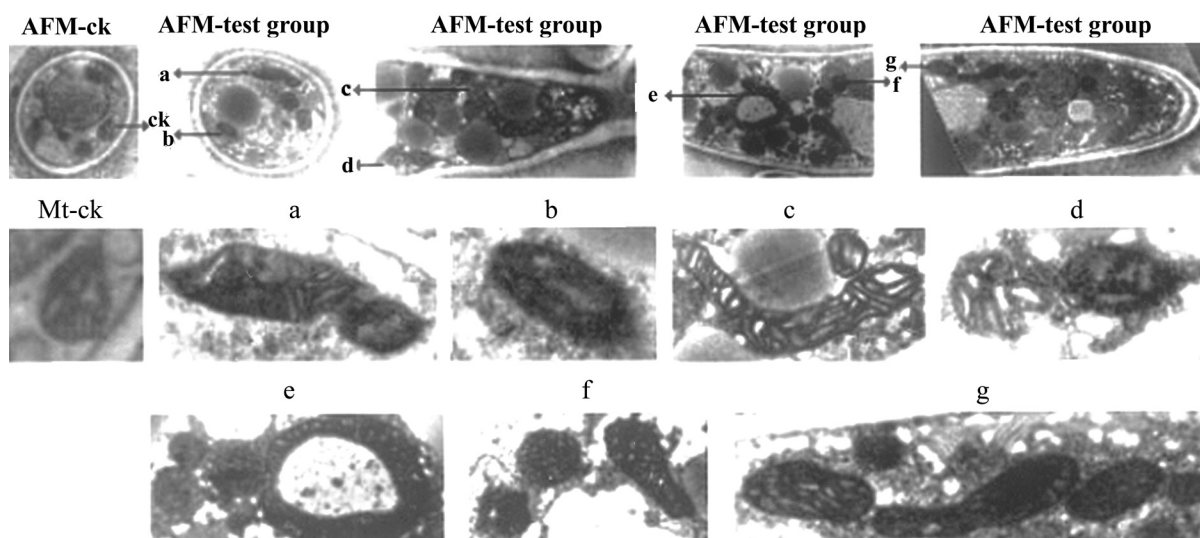


Fig. 4 Effects of citral on AFM's Mt in both number and shape

AFM-ck, *A. flavus* mycelium that germinated from normal conidia, and was cultured on PDA without citral at 29 °C for 5 d. AFM-test group, the *A. flavus* mycelium that germinated from conidia, which was treated by 0.5 mg/ml citral and then was cultured on PDA without citral at 29 °C for 5 d. Mt-ck, magnification ($\times 15,000$) of mitochondrion in *A. flavus* mycelium of AFM-ck; a, b, c, d, e, f and g, 4 times corresponding magnifications of mitochondrion in *A. flavus* mycelium of AFM-test group.

numbers and shapes.

Change of AFS photoabsorption

The absorption spectrum of a single living AFS at 350–750 nm is shown in Fig. 5. The spectrum of the test group was similar to that of the control group. Compared with the control group, the absorbance at 350–750 nm of the test groups increased. The absorbance integral values at 350–750 nm, 350–410 nm, 410–630 nm and 630–750 nm were calculated with multi-dimensional microscopy system. The following linear relationships were found between the absorbance integral value ($\Sigma\text{Abs.}$) and the concentration of citral:

for 350–750 nm: $\Sigma\text{Abs.}=207.54+33.14\times[\text{citral}]$
($r^2=0.96$, $P<0.001$);

for 350–410 nm: $\Sigma\text{Abs.}=103.00+17.76\times[\text{citral}]$
($r^2=0.92$, $P<0.01$);

for 410–630 nm: $\Sigma\text{Abs.}=47.02+7.96\times[\text{citral}]$
($r^2=0.97$, $P<0.001$);

for 630–750 nm: $\Sigma\text{Abs.}=61.58+6.76\times[\text{citral}]$
($r^2=0.96$, $P<0.001$).

There were two possible explanations for the increase of absorbance. The first was the increase of the total concentration of molecules in AFS, suggesting that the AFS volume became smaller. The second was the aggregation of the molecules entering from the outside of tested region. It is known that monomer A and B of citral absorbs the light of 230 nm and 330 nm, respectively [19], So citral itself could absorb no light at 350–750 nm. Therefore, citral is involved in the decrease of AFS volume and the aggregation of molecules in AFS.

Particle diameter size and its distribution in AFS

With quasi-elastic laser light scattering technique, the particle diameter size in AFS extract and its distribution were obtained (Table 1). It can be seen that there were 10 types of particles in the control group and their contents were more than 1%. The diameter size of particle with the

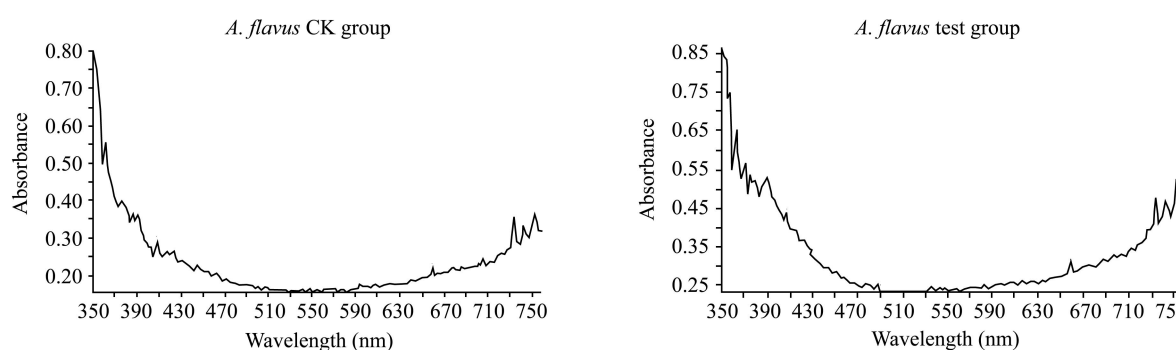


Fig. 5 Intracellular photoabsorption in a single AFS by MMSP

Table 1 Effects of citral on the particle diameter size in AFS extract and its distribution

Citral concentration (mg/ml)									
0 (Control group)		0 (Control group)		0 (Control group)		0 (Control group)		0 (Control group)	
D (nm)	Content (%)	D (nm)	Content (%)	D (nm)	Content (%)	D (nm)	Content (%)	D (nm)	Content (%)
51.46	85	72.34	76	73.86	78	76.31	65	84.14	68
54.86*	100	76.87	68	87.48*	100	89.78*	100	98.67*	100
58.48	80	81.68*	100	103.61	67	105.62	68	115.71	85
62.35	45	86.80	43	122.72	24	124.26	26	135.68	43
66.47	18	92.23	31	145.35	3	146.19	2	159.11	13
210.31	1	243.80	4	203.91	3	202.34	4	256.56	7
224.21	2	259.07	7	241.51	7	238.04	9	300.05	40
239.02	3	275.30	12	286.05	15	280.05	16	352.79	42
254.82	3	292.54	11	338.80	47	329.47	82	413.70	3
271.66	2	310.86	11	401.28	1	387.61	2	485.12	1

* indicated the soluble particle with the highest content, which was set to 100%.

largest content was 54.86 nm. Since its diameter size fell within the range of colloidal particle size (1–100 nm), the particle might be the main dispersal phase in the colloidal dispersion of AFS extract. It can be also seen from Table 1 that as the citral concentration increased, the diameter size of particle with the largest content increased also. Regression analysis showed that there was a better linear relationship between the diameter size and the concentration of citral ($D=53.79+9.57\times[\text{citral}]$, $r^2=0.83$, $P<0.05$), suggesting that citral is capable of inducing the aggregation of macromolecules in AFS.

Discussion

Concerning the effects of citral on physiological function of *A. flavus* cell, Luo *et al* reported that in the presence of citral, the electric conductivity of *A. flavus* membrane increased, the activity of $[\text{Na}^+, \text{K}^+]\text{-ATPase}$ of *A. flavus* membrane decreased, and the utilization rate of protein and sugar decreased [11]. But the correlative evidence of citral damage on cellular structure was rarely reported. In this paper, results from optical microscope and transmission electron microscope indicate that citral causes a direct damage to the AFS wall and membrane. The analysis of morphological parameters suggested that the decrease in AFS volume was related to citral. The volume-adjusting mechanisms need intact structure of the ion channel of transmembrane transport [20]. Therefore, the decrease in AFS volume reflects the weakening in volume-adjusting function of membrane. Non-invasive measurement on the elasticity parameters of AFS revealed that citral resulted in an increase in the membrane rigidity and a decrease in its flexibility. In order to explain this, thiobabutaric acid (TBA) colorimetry was used to detect malondialdehyde (MDA) content in AFS treated with citral. The TBA colorimetry experiment showed that citral resulted in an obvious increase of MDA content (data unpublished). MDA tends to interact with the amino group of membrane lipid and membrane proteins to increase the membrane rigidity and decrease its flexibility [21].

After entering the cell through its damaged membrane, citral affects the systems of biological oxidation and tricarboxylic acid cycle. Luo *et al.* [11] reported that with succinate, pyruvate and α -ketoglutarate as substrates, the respiratory rate and oxygen consumption of Mt, and the activity of malate dehydrogenase and succinate dehydrogenase decreased obviously. These data are in accordance with the observation of morphological structure under transmission electron microscope, implying that

the injury of its shape led to the decrease of Mt function. We have reported that citral damages the nuclear DNA of AFS [22]. The shape and quantitative change of Mt were caused by citral during sporing. Therefore, nuclear DNA injury in AFS might be involved in the genes related to Mt duplication and its morphogenesis.

Recently, more and more molecular biologists pay close attention to intracellular macromolecule crowding. There is a higher-ordered macromolecule crowding in cell [23]. It not only determines the conformation of all macromolecules and affects their association and dissociation [24,25], but also plays an important role in all biological processes relying on non-covalent union and/or conformational change (e.g. synthesis of protein and nucleic acid, intermediary metabolism, cell signals, genetic expression, and the function of dynamic motile systems) [26–31]. Our results from the non-invasive measurement of the morphological parameters and absorption of a living AFS showed that citral made AFS smaller, so the concentration of its macromolecules increased and they became overcrowded. In macromolecule overcrowding, a non-functional aggregation occurred, as shown in quasi-elastic laser light scattering. In conclusion, citral damages the structure of cell wall and membrane, leading to the loss of membrane functions. After entering the cell, citral not only influences the nucleus DNA and Mt, but also produces crowding, which causes non-functional aggregation of macromolecules, leading to metabolic disorder.

Acknowledgements

We would like to thank Dr. Mei TU, Dr. Tao JI, Dr. Jing LI and Dr. Cheng-Can YAO for assistance with experiments.

References

- 1 New Medical College of Jiangsu. Great Dictionary of Chinese Medicine. 1st ed. Shanghai People Publisher, 1977, 2: 1572–1573
- 2 Zhou J, Li PT. Research of antibacterial mechanism of *Litsea cubeba* oil in *staphylococcus aureus*. Bulletin of Hunan Medical University, 1992, 17(4): 329–332
- 3 Xia ZD, Yang JX, Li PT. Study on antifungal mechanism of *Litsea cubeba* oil in *Candida albicans*. Bulletin of Hunan Medical University, 1995, 20(2): 107–108
- 4 Zhou J. Progress in study on the pharmacology and clinical medicine of *Litsea cubeba* oil. Chinese Journal of Integrated Traditional and Western Medicine, 1991, 11(8): 509–512
- 5 Li KQ, Tang T. Study on effective composition of *Litsea cubeba* oils antifun-

- gal role. Chinese Journal Hospital Pharmacy, 1988, 6(11): 3–4
- 6 Huang-Liang YL, Su ML, Chen PR. The analysis of components of essential oil from fruit of *Litsea cubeba* and the study of antifungal activity/decay-free activity. Natural Product Research and Development, 1994, 6(4): 1–5
 - 7 Yu BL. Antibiotic activities of *Litsea cubeba* oil on moulds and effect of *Litsea Cubeba* oil on aflatoxin production. Microbiology, 1998, 25(3): 144–147
 - 8 Zhou Y, Tao JD, Zhang JJ. Study on the antifungal role by *Litsea cubeba* oil and its primary component—the citral. Chinese Journal of Integrated Traditional and Western Medicine, 1984, 4(9): 558–559
 - 9 Pattnaik S, Subramanyown VR, Bapaji M, Kole CR. Antibacterial and antifungal activity of aromatic constituents of essential oils. Microbios, 1997, 89(358): 39–46
 - 10 Zhou J, Li PT, Chen W. Study on antibacterial mechanism of *Litsea cubeba* oil in *Pseudomonas aeruginosa*. Bulletin of Hunan Medical University, 1993, 18(1): 33–35
 - 11 Luo M, Jiang LK, Wu ZJ. Preliminary study on citral impairs the *Aspergillus flavus*. Acta Microbiological Sinica, 2001, 41(6): 723–729
 - 12 Luo M, Jiang LK. Improvement on the purification method of *Litsea cubeba* oil. Wild Plant Resources, 1999, 18(3): 64–65
 - 13 Strey H, Peterson M, Sackmann E. Measurement of erythrocyte membrane elasticity by flicker eigenmode decomposition. Biophys J, 1995, 69: 478–488
 - 14 Li J, Huang YX, Ji T, Tan RC, Chen WX, Chen GW. Non-invasive measurement on the elasticity of red blood cell membrane with dynamic image analyzing technique. Acta Biophys Sin, 2002, 18(3): 351–354
 - 15 Huang YX, Ji T. The method and equipment of a fast multi-channel micro-spectrophotometer. Chinese Patent No. 00117473.8, G01N21/17, 2001
 - 16 Ji T, Chen GW, Chen WX, Huang YX. A novel fast multi-channel micro-spectrophotometer. Acta Biophys Sin, 2001, 17(3): 599–604
 - 17 Peng YG, Huang YX. Laser light scattering studies on flocculation. Environment Technology, 2001, 6: 42–45
 - 18 Luo M, Jiang LK. Study on biochemical mechanism of citral damper the *Aspergillus flavus* mitochondria. Acta Microbiolog Sin, 2002, 42(2): 226–231
 - 19 Information Center of Traditional Chinese Medicine, State Administration of Medicine and Drug (Guo Jia Yi Yao Guan Li Ju Zhong Cao Yao Qing Bao Zhong Xin). *Plant Medicine Effective Components Manual (Zhi Wu Yao You Xiao Cheng Fen Shou Ce)*. In: 0274 Citral. Beijing Public Health Publisher, 1986, 220–221
 - 20 Lang F, Busch GL, Ritter M, Volkl H, Waldegger S, Gulbins E, Haussinger D. Functional significance of cell volume regulatory mechanisms. Physiol Rev, 1998, 78: 247–306
 - 21 Hochstein P. *Lipid Peroxides in Biology and Medicine*. New York: Academic Press, 1982, 81
 - 22 Luo M, Huang YX, Jiang LK, Ji T, Tu M. Study on quantitative test on the DNA damage of *Aspergillus flavus* caused by citral with a comet analysis system. Acta Microbiologi Sin, 2002b, 42(3): 341–347
 - 23 Minton AP. The effect of volume occupancy upon the thermodynamic activity of proteins: Some biochemical consequences. Mol Cell Biochem, 1983, 55: 119–140
 - 24 Zimmerman SB, Minton AP. Macromolecule crowding: Biochemical, biophysical and physiological consequences. Annu Rev Biophys Biomol Struct, 1993, 22: 27–65
 - 25 Ellis RJ. Macromolecule crowding: An important but neglected aspect of the intracellular environment. Curr Opin Struct Biol, 2001, 11(1): 114–119
 - 26 Ellis RJ. Macromolecular crowding: Obvious but underappreciated. Trends Biochem Sci, 2001, 26(10): 597–604
 - 27 Minton AP. The influence of macromolecular crowding and macromolecular confinement on biochemical reactions in physiological media. J Biol Chem, 2001, 276: 10577–10580
 - 28 Minton AP. Implications of macromolecular crowding for protein assembly. Curr Opin Struct Biol, 2000, 10(1): 34–39
 - 29 van den Berg B, Ellis R, Dobson CM. Effects of macromolecular crowding on protein folding and aggregation. EMBO J, 1999, 18: 6927–6933
 - 30 van den Berg B, Wain R, Dobson CM, Ellis R. Macromolecular crowding perturbs protein refolding kinetics: Implications for folding inside the cell. EMBO J, 2000, 19: 3870–3875
 - 31 Martin J, Hartl FU. The effect of macromolecular crowding on chaperonin-mediated protein folding. Proc Natl Acad Sci USA, 1997, 94: 1107–1112

Edited by
You-Shang ZHANG